

Some Closed-Form Results for Adhesive Rough Contacts Near Complete Contact on Loading and Unloading in the Johnson, Kendall, and Roberts Regime

Michele Ciavarella

Center of Excellence in
Computational Mechanics,
Politecnico di BARI,
Viale Gentile 182,
Bari 70126, Italy
e-mail: Mciava@poliba.it

Yang Xu

Mechanical Engineering Department,
Auburn University,
Auburn, AL 36849

Robert L. Jackson

Mechanical Engineering Department,
Auburn University,
Auburn, AL 36849

Recently, generalizing the solution of the adhesiveless random rough contact proposed by Xu, Jackson, and Marghitu (XJM model), the first author has obtained a model for adhesive contact near full contact, under the Johnson, Kendall, and Roberts (JKR) assumptions, which leads to quite strong effect of the fractal dimension. We extend here the results with closed-form equations, including both loading and unloading which were not previously discussed, showing that the conclusions are confirmed. A large effect of hysteresis is found, as was expected. The solution is therefore competitive with Persson's JKR solution, at least in the range of nearly full contact, with an enormous advantage in terms of simplicity. Two examples of real surfaces are discussed.

[DOI: 10.1115/1.4036915]

Keywords: Greenwood–Williamson (GW) model, roughness, adhesion, hysteresis, fractals

1 Introduction

Adhesion between elastic rough bodies is still not well understood, probably because between the theory of elastic contact (Hertz theory, late 1880s, see Ref. [1]) and the first paper on adhesion of elastic spheres (due to Johnson, Kendall, and Roberts [2], the JKR theory), there is almost a century. Also, contact of elastic rough surfaces is only recently being understood with accuracy, and the first famous “asperity” model again is only 50 yr old [3]. Greenwood and Williamson (GW) were extended to adhesion in each single isolated asperities by Fuller and Tabor [4] which qualitatively seemed to justify the main intuitive result: adhesion is destroyed by small “amounts” of amplitude of roughness.

Before discussing the complex case of adhesion of rough surfaces, we may recollect that it took a few decades to just understand the role of different parameters in the simple case of a spherical contact. Indeed, Bradley [5] and Derjaguin [6] have obtained the adhesive force between two *rigid* spheres, equal to $2\pi R w$, where w is the work of adhesion, and R is the radius of the sphere, but only JKR [2] developed a theory for elastic spheres, obtaining 3/4 of the Bradley pull-off value, whereas a few years later Derjaguin, Muller, and Toporov (DMT) proposed a theory [7], which returned to the Bradley value. Only Tabor explained that the two theories applied at the extremes of a dimensionless parameter [8]

$$\mu = \left(\frac{R w^2}{E^* \Delta r^3} \right)^{1/3} = \frac{(R l_a^2)^{1/3}}{\Delta r} = \frac{\sigma_{th}}{E^*} \left(\frac{R}{l_a} \right)^{1/3} \rightarrow 0 \quad (1)$$

where Δr is the equilibrium distance of atoms, and E^* is the plane strain elastic modulus. Also, we have introduced the length

$l_a = w/E^*$ as an alternative measure of adhesion, and σ_{th} is the theoretical strength of the material.

With rough surface contact, apart from the early attempt by Fuller and Tabor [4], only recently Persson [9] and Persson and Scaraggi [10] have attempted semi-analytical theories. Persson [9] was originally aimed at the JKR regime and, apart from its extreme complexity, it has not received independent validation with numerical experiments, and more importantly, it does not seem to contain any irreversible process, which does not make clear the order of approximations made and the predicting capabilities in a regime which is expected to be strongly hysteretic.¹ Persson and Scaraggi [10], instead, aim at the DMT regime which they predict is completely reversible (there is only a single loading–unloading curve), and attempt to define “multiscale” versions of the DMT parameter, but they offer only a limited set of results.

The main features of the JKR regime appear clearly already in the relatively simple behavior of a single sinusoidal contact [12]. Taking therefore a sinusoid (in either one-dimensional (1D) or full two-dimensional (2D)) with λ wavelength, h amplitude, and considering the limiting case without adhesion, then $p^* = \pi E^* (h/\lambda)$ is the compressive mean pressure to flatten the 1D sinusoid if $\lambda = \lambda_x$ and 2D sinusoid if $\lambda = \sqrt{\lambda_x^2 + \lambda_y^2}$. For 1D adhesive waviness, for example, the solution depends on a parameter, Johnson's parameter [12]

$$\alpha = \sqrt{\frac{2\lambda w}{\pi^2 h^2 E^*}} \quad (2)$$

¹Krick et al. [11] seem to be in the best possible condition to check Persson's theory, but their experiments are discussed only quite qualitatively, perhaps because of the spherical geometry of contact. In any case, the experimental hysteresis in loading/unloading is justified by an argument of the effective interfacial energy being very different on loading and unloading, which is not included in Persson's theory.

Contributed by the Tribology Division of ASME for publication in the JOURNAL OF TRIBOLOGY. Manuscript received December 26, 2016; final manuscript received April 27, 2017; published online July 21, 2017. Assoc. Editor: James R. Barber.

In particular, the loading curve shows two extremes, a minimum and a maximum, which correspond to jump instabilities: under zero load, the contact jumps into an intermediate state, and under sufficient pressure, it jumps to full contact, where it shows a strength close to the theoretical stress of the material, unless we resort to postulating the existence of some flaw of trapped air, as Johnson suggests [12] and other impurities on the surface. For $\alpha > 0.57$, the surfaces will spontaneously snap into contact at zero load.

When translating this into the case of rough surfaces, it is clear that many gaps exist and many instabilities can occur. A very simplified case of roughness is that offered by Guduru [13], where roughness has a single scale over an otherwise spherical contact, and the main results have been confirmed experimentally [14], whereas Waters et al. [15] have also shown that the enhancement mainly holds under the JKR regime.

In the present paper, we shall further elaborate on the results of Ciavarella [16], obtaining some closed-form results for both loading and unloading for a regime near full contact, under JKR conditions.

2 The Model

In XJM [17], a model with the solution near full contact for a rough surface was obtained using the idea of pressurized gaps which Johnson [1] used for the 1D/2D sinusoid problem without adhesion, and then Johnson [12] used for the same problem with adhesion. Ciavarella [18] has derived further simplifications of the XJM model and shown, for example, that it leads exactly to Persson [19] well-known approximate solution, if a “bearing area” is used to estimate the noncontact area from the full contact pressure, and a corrective factor 4/3 is used for the noncontact area. Ciavarella [16] has extended this solution for the JKR adhesive case, limited to loading conditions, under further small approximations. This solution is relatively easy to extend for unloading.

The main idea is approximating the distributions of tensile stresses in the gaps by means of parabolic equations (similarly to what is done in asperity theories in approximating the asperity summit geometries, so that all the results of the classical random process theory hold). We notice however that we are by no means approximating the real rough surface with asperities, as done in the classical GW model and therefore our model has nothing to do with the Fuller and Tabor model using asperities.

This leads to the following (see Refs. [16–18] for more details) expression for the noncontact area, A_{nc} (normalized by the nominal contact area A_0):

$$\frac{A_{nc}(\bar{p})}{A_0} = 3\pi R^p \eta \int_{\bar{p}}^{\infty} (p - \bar{p}) \Phi(p) dp \quad (3)$$

where R^p and η are the radius and the density of the full contact pressure “surface” asperities, $\Phi(p)$ the probability density of their heights (mean level does not correspond strictly to zero, but is displaced by a quantity m^p according to classical random theory process, see Ref. [20]), and hence it can be solved easily. Notice that the integral is simply of the same mathematical form as in the standard Greenwood and Williamson’s theory, where mean separation is replaced by mean pressure, and the geometrical surface is replaced by the full contact pressure surface. However, one more time we remark that our result has nothing to do with simulating the real surface with asperities.

From Ref. [20]

$$\begin{aligned} \eta^p &= \frac{1}{6\sqrt{3}\pi} \frac{m_4^p}{m_2^p}, & R^p &= 0.375 \sqrt{\frac{\pi}{m_4^p}}, \\ \sigma_s^p &= \sqrt{1 - \frac{0.9}{\alpha^p}} \sqrt{m_0^p}, & m^p &= 4 \sqrt{\frac{m_0^p}{\pi \alpha^p}} \end{aligned} \quad (4)$$

where the superscript “ p ” stands to quantities relative to the full contact pressure surface. The general definition of the (even order)

moments is reduced into the following form [21] if the power spectrum density (PSD), $C(q)$, is axisymmetric (e.g., the rough surface is isotropic), where $q = 2\pi/\lambda$ is wavevector:

$$m_n = m_{n0} = \int_{q_0}^{q_1} \int_0^{2\pi} [q \cos(\theta)]^n C(q) q dq d\theta = T(n) \int_{q_0}^{q_1} C(q) q^{n+1} dq \quad (5)$$

where $T(n) = 2\pi, \pi, 3/4\pi$ ($n = 0, 2, 4$).

The full contact pressure moments m_{2n}^p , then, considering the transfer function between the PSD of the roughness and the corresponding full contact pressure surface is simply $(E^*/2)^2 q^2$, are [16,21]

$$m_0^p = \frac{1}{2} E^{*2} m_2, \quad m_2^p = \frac{1}{3} E^{*2} m_4, \quad m_4^p = \frac{3}{10} E^{*2} m_6 \quad (6)$$

Therefore, the moment m_4^p is related to the moment m_2 and so on. Also, $\alpha^p = m_0^p m_4^p / (m_2^p)^2 = (27/20) m_2 m_6 / (m_0)^2$ is the bandwidth parameter [22] for the full contact pressure surface and is generally much lower than Nayak parameter α for the rough surface itself.² Finally, the root-mean-square (RMS) height of the asperity of the full contact pressure surface is σ_s^p a little smaller than $\sqrt{m_0^p}$. Therefore (here we differ from Refs. [16] and [18] in that we take in more precise account of the GW parameters)

$$\Phi(p) = \frac{1}{\sqrt{2\pi}\sigma_s^p} \exp\left(-\left(\frac{p - m^p}{\sqrt{2}\sigma_s^p}\right)^2\right) \quad (7)$$

and moving to a dimensionless notation $p' = p/\sigma_s^p$ and a dimensionless $\Phi' = \sigma_s^p \Phi$, we have

$$\frac{A_{nc}(\bar{p}')}{A_0} = 3\pi R^p \eta^p \sigma_s^p \int_{\bar{p}'}^{\infty} (p' - \bar{p}') \Phi'(p') dp' \quad (8)$$

where $\bar{p}' = \bar{p}/\sigma_s^p$. Notice that with the McCool parameters

$$R^p \eta^p \sigma_s^p \simeq 0.02 \sqrt{\alpha^p}$$

In the present form, we obtain

$$\begin{aligned} \frac{A_{nc}(\bar{p}')}{A_0} &= 0.06\pi \sqrt{\alpha^p} \left[\frac{1}{\sqrt{2\pi}} \exp\left[-\left(\frac{\bar{p}' - m^{p'}}{2}\right)^2\right] \right. \\ &\quad \left. - \frac{1}{2} (\bar{p}' - m^{p'}) \operatorname{Erfc}\left(\frac{(\bar{p}' - m^{p'})'}{\sqrt{2}}\right) \right] \end{aligned} \quad (9)$$

where now $m^{p'} = m^p/\sigma_s^p = 4\sqrt{1/(\pi\alpha^p)}/\sqrt{1 - (0.9/\alpha^p)}$. Notice that this equation was not derived by Ref. [6] nor [21].

We shall see that this curve is extremely close to the Persson [19] solution for a large range of α^p , where we normalize as in Persson, by the RMS full contact pressure, $\bar{p}'' = \bar{p}/\sqrt{m_0^p}$

$$\frac{A_{nc}(\bar{p}'')}{A_0} = \operatorname{Erfc}\left(\bar{p}''/\sqrt{2}\right) \quad (10)$$

This was explained qualitatively with a bearing area argument in Ref. [18], but it is here found more in details from the GW argument,

²The error in classical asperity theories can be considerable and depends on the Nayak bandwidth (at least for the area load, see Ref. [23]), whereas in the “full contact pressure” asperity theory here discussed the results, in the adhesionless case, will be extremely close to Persson’s theory [19], and almost independent on the “full contact pressure” bandwidth parameter α^p , as we shall explain.

which assumes equal radius for all pressure asperities, but is also confirmed by more elaborate theories derived by Xu et al. [17,21].

The effect of α^p is relatively small, and Ref. [21] seems to suggest the GW model to be more accurate than Persson's solution in the range near full contact (Fig. 1).

2.1 The Johnson, Kendall, and Roberts Adhesive Case. We have shown in Ref. [16] that, under a small approximation of the JKR curve of the gaps (see Fig. 2 of Ref. [16])—where it is evident that the following approximation will slightly overestimate the noncontact area), the integral becomes (returning to dimensional variables):

$$\frac{A_{nc}(\bar{p})}{A_0} = 3\pi R^p \eta^p \int_{\bar{p}+p_0}^{\infty} \left(p - \left(\bar{p} + \frac{1}{2} p_0 \right) \right) \Phi(p) dp \quad (11)$$

$$\frac{A_{nc}(\bar{p}')}{A_0} = 0.06\pi\sqrt{\alpha^p} \left(\begin{array}{l} \frac{1}{\sqrt{2\pi}} \exp \left[- \left(\frac{(\bar{p}' + p'_0 - m^{p'})^2}{2} \right) \right] \\ - \frac{1}{2} \left(\bar{p}' + \frac{1}{2} p'_0 - m^{p'} \right) \operatorname{Erfc} \left(\frac{(\bar{p}' + p'_0 - m^{p'})'}{\sqrt{2}} \right) \end{array} \right) \quad (13)$$

and a comparison with the adhesionless solution shows that the p'_0 term is not added to the mean pressure in all the terms. We cannot avoid plotting different curves with respect to the adhesionless scale, as in the existing solution in Ref. [16] which is more approximate. We shall plot curves however together with unloading one, as soon as we obtain the solution of this case in the following paragraph.

2.2 Unloading. We add now the treatment for unloading of a JKR contact. Suppose we load up to \bar{p}_{max}' , some contacts will jump irreversibly into full contact, and others instead can enlarge again as soon as load is reduced: eliminating the first component gives

$$\frac{A_{nc}^{unload}(\bar{p})}{A_0} = 3\pi R^p \eta^p \int_{\bar{p}_{max}+p_0}^{\infty} \left(p - \left(\bar{p} + \frac{1}{2} p_0 \right) \right) \Phi(p) dp \quad (14)$$

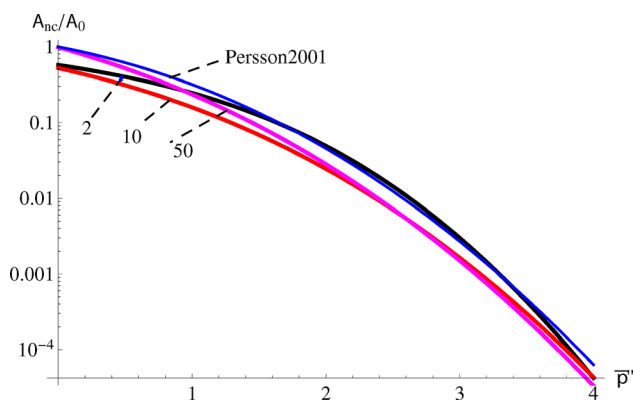


Fig. 1 Adhesionless contact. The area of gaps ($A_{nc}(\bar{p}')/A_0$) as a function of applied pressure for $\alpha^p = 2, 10, 50$ (black, red, and magenta curves), where pressure is normalized to RMS full contact pressure, as compared with Persson's solution (blue solid line).

where we find both in the integrand and in the extreme of integration, the mean pressure increased depending on a factor

$$p_0 = \psi \left(\frac{K_{Ic}^4}{R_p} \right)^{1/5} \quad (12)$$

where $\psi = (1/3((3/8)\sqrt{\pi})^{4/5} + \sqrt{\pi}/(2((3/8)\sqrt{\pi})^{1/5})) = 1.20$, and K_{Ic} is toughness of the contact. Notice that there is an error of a factor 1/2 in Ref. [16] which does not permit (strictly speaking) the simplification we made there to replace the mean pressure by the p_0 term.

However, the integration can be done also with adhesion

Also, this can be given in closed-form as

$$\frac{A_{nc}^{unload}(\bar{p} < \bar{p}_{max}')}{A_0} = \frac{0.06\pi}{\sqrt{2\pi}} \sqrt{\alpha^p} \left\{ \exp \left[- \left(\frac{(\bar{p}'_{max} + p'_0 - m^{p'})^2}{2} \right) \right] - \sqrt{\frac{\pi}{2}} \left(\bar{p}' + \frac{1}{2} p'_0 - m^{p'} \right) \times \operatorname{Erfc} \left(\frac{(\bar{p}'_{max} + p'_0 - m^{p'})}{\sqrt{2}} \right) \right\} \quad (15)$$

Results are plotted in Fig. 2 for $p'_0 = p_0/\sqrt{m_0^p} = 1$ and $\alpha^p = 2$. Unloading curves from $\bar{p}'_{max} = \bar{p}'_{max}/\sqrt{m_0^p} = 1, 2$ are shown with dashed lines, whereas the “Persson-like” solution of Ciavarella [16] which we consider an approximation is shown in blue solid line. It can be seen that unloading returns only a small fraction of contacts, if the squeezing pressure had gone quite large.

Naturally, when $p'_0 \gg 0$, the area of noncontact is very small already at near zero pressure, which indicates that the solution is

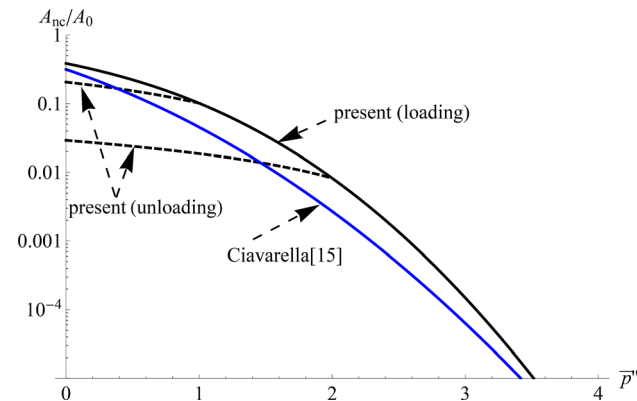


Fig. 2 The area of gaps ($A_{nc}(\bar{p}')/A_0$) as a function of applied pressure and for $p'_0 = 1$ and $\alpha^p = 2$, where pressure is normalized to RMS full contact pressure. Blue solid line is Persson's “shifted” solution of Ciavarella [15], black solid line is the present solution, and dashed lines are unloading curves from $\bar{p}'_{max} = 1, 2$.

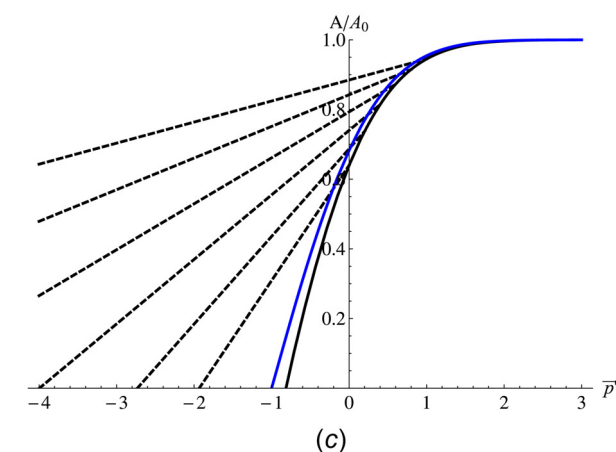
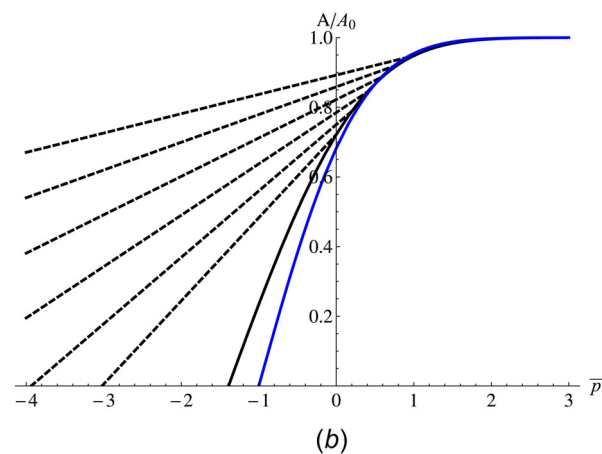
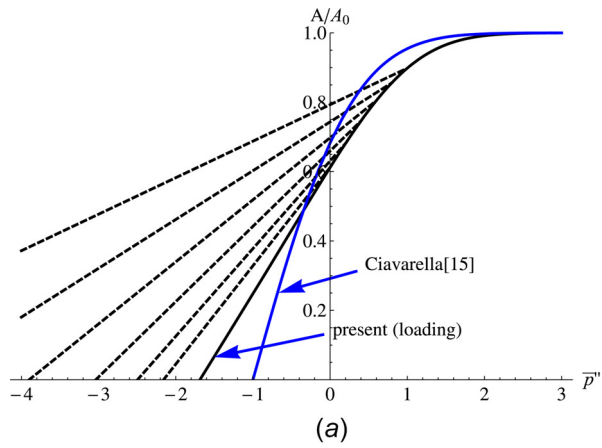


Fig. 3 Area of contact for $\alpha^p = 2, 10, 50$ (a)–(c), for $p_0' = 0.01$ and unloading curves from $\bar{p}_{\max}'' = 0.2, \dots, 1$

less and less useful, because our intrinsic assumption in approximating the pressure as parabolic distribution from the summits of the full contact pressure surface requires that the mean pressure itself to be sufficiently high.

It may be perhaps more interesting to draw plots for the normalized contact area $1 - (A_{nc}/A_0)$, as in Fig. 3, where it is evident that the unloading curves are almost linear in pressure. It seems that the Persson-like shifted solution of Ciavarella [16] is a good approximation at high α^p , and otherwise there is a significant deviation.

One may obtain by extrapolation the value for which the area goes to zero

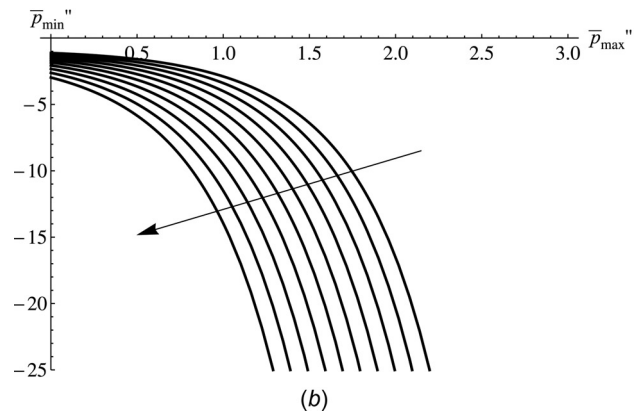
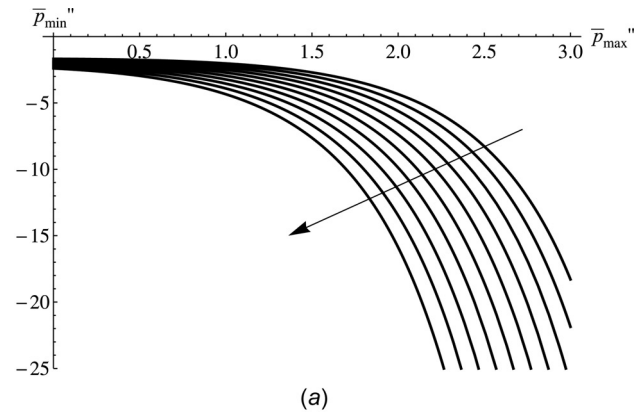


Fig. 4 Pull-off value extrapolated as pressure for which area of contact $(A(\bar{p}''))/A_0$ on unloading seems to go to zero, depending on the pressure reaches during loading \bar{p}_{\max}'' . The arrow indicates $p_0' = 0.1, 0.2, \dots, 1$. (a) $\alpha^p = 2$ and (b) $\alpha^p = 10$.

$$\bar{p}'_{\min} = m p_0' - \frac{1}{2} p_0' + \sqrt{\frac{2}{\pi}} \frac{\exp\left[-\left(\frac{\bar{p}'_{\max} + p_0' - m p_0'}{2}\right)^2\right]}{\operatorname{Erfc}\left(\frac{\bar{p}'_{\max} + p_0' - m p_0'}{\sqrt{2}}\right)} - \frac{\sqrt{2\pi}}{0.06\pi\sqrt{\alpha^p}} \quad (16)$$

which is tempting to define “pull-off,” but obviously it is only vaguely related to it since the model assumes we are near full contact.

Plotting actual values in Fig. 4, it is clear that the model extrapolates to a pull-off which is nonlinear function of the maximum pressure, and that it does not go to the correct limit of zero for negligible adhesion, for the simple reason that it extrapolates from full contact.

Moreover, all the conclusions in Ref. [16] are still valid, as the increase of \bar{p}'_0 leads to a paradoxical behavior similar to that discussed by Johnson [12] for the JKR solution of a single sinusoid—once full contact is achieved, JKR model gives a very high limit for pull-off, which may be questionable in the presence of contaminants, trapped air, finite elasticity, cohesive forces, etc.

3 Application to Rough Self-Affine Surfaces

Turning back to our adhesion problem, Persson [9] theory, as well as Afferrante et al. [24] for deterministic Weierstrass, seems to conclude that the contact area should lead to some limit in the “fractal limit,” not depending on truncating wavelength. Here, as in Ref. [16], we find that we can find open gaps for $p - \bar{p} > p_0$ during the loading stage, where p_0 is a characteristic pressure

which depends on the characteristic length of adhesion l_a and on m_6 , the sixth moment of the surface PSD, as

$$p_0 = 1.2 \left(\frac{K_{Ic}^4}{R^p} \right)^{1/5} = 1.523 E^{*3/5} w^{2/5} m_6^{1/10}$$

or in dimensionless form

$$p_0'' = p_0 / \sqrt{m_0''} = 1.523 \sqrt{2} \frac{m_6^{1/10}}{m_2^{1/2}} l_a^{2/5}$$

When p_0'' is large (p_0 comparable to the RMS full contact pressure), this leads to a limit solution extremely close to full contact, but the assumptions are really in contrast with the approximation of quadratic pressure distribution, i.e., of “low” pressure asperities, which requires $\bar{p} \gg p_0$. In other words, Ciavarella [16] and the present variant solution really should be taken as a first-order correction of the adhesionless counterparts for low p_0'' .

For typical self-affine surfaces, the power spectrum is a power law above a certain long wavelength cutoff (wavenumber q_0)

$$C(q) = \begin{cases} 0 & \text{for } q < q_0 \\ Zq^{-2(H+1)} & \text{for } q_0 < q < q_1 \\ 0 & \text{for } q > q_1 \end{cases} \quad (17)$$

where $q_1 = \zeta q_0$ could be a real finite short wavelength cutoff, or just a measurement cutoff—in which case often the term “magnification ratio” is introduced as ζ . The constant Z can be determined by the prescribed RMS height, $h_{rms} = \sqrt{m_0}$, of the roughness based on Eq. (5): $m_0 = 2\pi \int_{q_0}^{q_1} Z q^{-2H-1} dq = (\pi Z/H) (q_0^{-2H} - q_1^{-2H}) \simeq (\pi Z/H) q_0^{-2H} = (\pi/H) C(q_0) q_0^2$

$$Z \simeq \frac{H}{\pi} h_{rms}^2 q_0^{2H}$$

As it is well known, only m_0 is truly bounded (the variance of the heights) in the sense that it is defined mainly at the coarse scales, whereas m_2 diverges as well as the other higher-order ones, including the very high moment m_6 , on which the present theory is based. Hence, even for very low fractal dimensions, the problem remains sensitive to truncation.

For actual comparison unfortunately, there are not many data available on adhesive rough contacts, as the problem is probably still computationally demanding, and the only one, the 1D results of Carbone et al. [25], does not satisfy our requirement, $p_0'' \ll 1$ (see the Appendix). This is because the data are relative to a very low modulus material with significant adhesion, therefore depart too much from the adhesionless condition, and moreover are not pushed near full contact (the highest contact area seems to be near 0.4).

4 Conclusion

A closed-form result has been derived for both the adhesionless and adhesive contact between random rough surfaces, under JKR conditions, and assuming adhesion is not too strong. In the latter case, this includes also the unloading regime, which shows a large hysteresis. We obtain results that, for some realistic surfaces as we show from two examples, predict either very strong adhesion or very small departure from the adhesionless solution. There remains a theoretical problem about the fractal limit and sensitivity to truncation of the measurement. What would be the meaning of the model at, say, atomic scale?

Appendix: The Data in Carbone et al. [25]

As we want to compare with the JKR results with 1D surfaces of Carbone et al. [25], we reobtain the transfer of full contact pressure to surface moments in 1D. The K_I solution in 2D differs only by 6% from the three-dimensional crack solution for parabolic pressure, so it is not worth correcting for this factor.

Table 1 Values of p_0'' for the data in Ref. [25]

	$w = 0.01 \text{ J m}^{-2}$	0.04 J m^{-2}	0.07 J m^{-2}
$m_2 = 1.5 \times 10^{-3} (H = 0.9)$	3.4	5.9	7.4
$m_2 = 2.7 \times 10^{-3} (H = 0.8)$	2.9	5	6.25

From the general definition of the spectral moments in 1D

$$m_{2n} = \int_0^\infty C_{1D}(q) q^{2n} dq \quad (A1)$$

for the full contact pressure moments m_{2n}'' , considering the transfer function is simply $(E^*/2)^2 q^2$, we get

$$m_{2n}'' = (E^*/2)^2 \int_0^\infty C_{1D}(q) q^{2n+2} dq = (E^*/2)^2 m_{2(n+1)} \quad (A2)$$

Consider a self-affine 1D profile with Hurst exponent H , i.e., a power law PSD $C_{1D}(q) = Zq^{-(2H+1)}$. Computing the integrals, for sufficiently large magnifications, and $n > 0$, moments depend only on the high wavevector tail, and hence, for example,

$$\frac{m_6}{m_2} = \frac{2 - 2H}{6 - 2H} q_s^4, \quad m_2 = \frac{Z}{2 - 2H} q_s^{2-2H}$$

In Ref. [25], $k_s = 1000 k_0 = 1000 \text{ mm}^{-1}$, and hence $m_6 = ((2 - 2H)/(6 - 2H)) 10^{12} m_2 (\text{mm}^{-4})$, where $m_2 = 1.5 \times 10^{-3} (H = 0.9)$ or $2.7 \times 10^{-3} (H = 0.8)$, and so $m_6 = ((2 - 2 \cdot 0.9)/(6 - 2 \cdot 0.9)) 10^{12} \cdot 1.5 \times 10^{-3} = 7.143 \times 10^7 (\text{mm}^{-4})$ or $m_6 = ((2 - 2 \cdot 0.8)/(6 - 2 \cdot 0.8)) 10^{12} \cdot 2.7 \times 10^{-3} = 2.45 \times 10^8 (\text{mm}^{-4})$. Now, the critical minimum pressure defined in Ref. [16], using $R_p = 2/\sqrt{m_4''} = 2/\sqrt{m_4''} = 2/\sqrt{(E^*/2)^2 m_6} = 2/[(E^*/2)\sqrt{m_6}]$ and $K_{Ic}^2 = 2E^*w$

$$p_0'' = \frac{1.2(E^{*3} w^2 \sqrt{m_6})^{1/5}}{(E^*/2)\sqrt{m_2}} = 2.4 \frac{w^{2/5} m_6^{1/10}}{E^{*2/5} \sqrt{m_2}}$$

where $E^* = 1/(1 - 0.25^2) = 1.07 \text{ MPa}$ and $w = 0.01, 0.04, 0.07 \text{ J/m}^2$. Table 1 shows that the resulting p_0'' are very high.

References

- [1] Johnson, K. L., 1985, *Contact Mechanics*, Cambridge University Press, Cambridge, UK.
- [2] Johnson, K. L., Kendall, K., and Roberts, A. D., 1971, “Surface Energy and the Contact of Elastic Solids,” *Proc. R. Soc. London A*, **324**(1558), pp. 301–313.
- [3] Greenwood, J. A., and Williamson, J. B. P., 1966, “Contact of Nominally Flat Surfaces,” *Proc. R. Soc. London A*, **295**(1442), pp. 300–319.
- [4] Fuller, K. N. G., and Tabor, D., 1975, “The Effect of Surface Roughness on the Adhesion of Elastic Solids,” *Proc. R. Soc. London A*, **345**(1642), pp. 327–342.
- [5] Bradley, R. S., 1932, “The Cohesive Force Between Solid Surfaces and the Surface Energy of Solids,” *Philos. Mag.*, **13**(86), pp. 853–862.
- [6] Derjaguin, B. V., 1934, “Theorie des Anhaftens kleiner Teilchen,” *Kolloid Z.*, **69**(2), pp. 155–164.
- [7] Derjaguin, B. V., Muller, V. M., and Toporov, Yu. P., 1975, “Effect of Contact Deformations on the Adhesion of Particles,” *J. Colloid Interface Sci.*, **53**(2), pp. 314–326.
- [8] Tabor, D., 1977, “Surface Forces and Surface Interactions,” *J. Colloid Interface Sci.*, **58**(1), pp. 2–13.
- [9] Persson, B. N. J., 2002, “Adhesion Between an Elastic Body and a Randomly Rough Hard Surface,” *Eur. Phys. J. E*, **8**(4), pp. 385–401.
- [10] Persson, B. N. J., and Scaraggi, M., 2014, “Theory of Adhesion: Role of Surface Roughness,” *J. Chem. Phys.*, **141**(12), p. 124701.
- [11] Krick, B. A., Vail, J. R., Persson, B. N., and Sawyer, W. G., 2012, “Optical In Situ Micro Tribometer for Analysis of Real Contact Area for Contact Mechanics, Adhesion, and Sliding Experiments,” *Tribol. Lett.*, **45**(1), pp. 185–194.
- [12] Johnson, K. L., 1995, “The Adhesion of Two Elastic Bodies With Slightly Wavy Surfaces,” *Int. J. Solids Struct.*, **32**(3–4), pp. 423–430.
- [13] Guduru, P. R., 2007, “Detachment of a Rigid Solid From an Elastic Wavy Surface: Theory,” *J. Mech. Phys. Solids*, **55**(3), pp. 445–472.
- [14] Guduru, P. R., and Bull, C., 2007, “Detachment of a Rigid Solid From an Elastic Wavy Surface: Experiments,” *J. Mech. Phys. Solids*, **55**(3), pp. 473–488.
- [15] Waters, J. F., Lee, S., and Guduru, P. R., 2009, “Mechanics of Axisymmetric Wavy Surface Adhesion: JKR–DMT Transition Solution,” *Int. J. Solids Struct.*, **46**(5), pp. 1033–1042.

- [16] Ciavarella, M., 2015, "Adhesive Rough Contacts Near Complete Contact," *Int. J. Mech. Sci.*, **104**, pp. 104–111.
- [17] Xu, Y., Jackson, R. L., and Marghitu, D. B., 2014, "Statistical Model of Nearly Complete Elastic Rough Surface Contact," *Int. J. Solids Struct.*, **51**(5), pp. 1075–1088.
- [18] Ciavarella, M., 2016, "Rough Contacts Near Full Contact With a Very Simple Asperity Model," *Tribol. Int.*, **93**(Pt. A), pp. 464–469.
- [19] Persson, B. N. J., 2001, "Theory of Rubber Friction and Contact Mechanics," *J. Chem. Phys.*, **115**(8), pp. 3840–3861.
- [20] McCool, J. I., 1987, "Relating Profile Instrument Measurements to the Functional Performance of Rough Surfaces," *ASME J. Tribol.*, **109**(2), pp. 264–270.
- [21] Xu, Y., and Jackson, R. L., 2017, "Statistical Models of Nearly Complete Elastic Rough Surface Contact-Comparison With Numerical Solutions," *Tribol. Int.*, **105**, pp. 274–291.
- [22] Nayak, P. R., 1973, "Random Process Model of Rough Surfaces in Plastic Contact," *Wear*, **26**(3), pp. 305–333.
- [23] Carbone, G., and Bottiglione, F., 2015, "Asperity Contact Theories: Do They Predict Linearity Between Contact Area and Load?" *J. Mech. Phys. Solids*, **56**(8), pp. 2555–2572.
- [24] Afferrante, L., Ciavarella, M., and Demelio, G., 2015, "Adhesive Contact of the Weierstrass Profile," *Proc. R. Soc. A*, **471**(2182), p. 20150248.
- [25] Carbone, G., Pierro, E., and Recchia, G., 2015, "Loading-Unloading Hysteresis Loop of Randomly Rough Adhesive Contacts," *Phys. Rev. E*, **92**(6), p. 062404.